



## Original Article

## Atomic displacement cross-sections for neutron irradiation of materials from Be to Bi calculated using the arc-dpa model

A. Yu. Konobeyev\*, U. Fischer, S.P. Simakov

Institute for Neutron Physics and Reactor Technology, Karlsruhe Institute of Technology, 76344 Eggenstein-Leopoldshafen, Germany



## ARTICLE INFO

## Article history:

Received 25 May 2018

Received in revised form

1 August 2018

Accepted 4 September 2018

Available online 7 September 2018

## Keywords:

Radiation damage

Displacement cross-section

Neutron irradiation

## ABSTRACT

Displacement cross-sections for an advanced assessment of radiation damage rates were obtained for a number of materials using the arc-dpa model at neutron incident energies from  $10^{-5}$  eV to 10 GeV. Evaluated data files, CEM03 and ECIS codes, and an approximate approach were applied for the calculation of recoil energy distributions in neutron induced reactions.

Three sets of displacement cross-sections based on the use of low-energy data from JEFF-3.3, ENDF/B-VIII.0, and JENDL-4.0u were prepared. Files contain also cross-sections calculated using the standard NRT model.

Special efforts were made to estimate the uncertainty of obtained displacement cross-sections.

© 2018 Korean Nuclear Society, Published by Elsevier Korea LLC. This is an open access article under the CC BY-NC-ND license (<http://creativecommons.org/licenses/by-nc-nd/4.0/>).

## 1. Introduction

Obtaining reliable displacement cross-sections is an essential prerequisite for the correct calculation of the radiation damage rate in materials. The application of neutron displacement cross sections concerns all types of nuclear facilities, including fission and fusion reactors, accelerators, and spallation sources.

The use of the standard NRT model [1,2] for the calculation of the number of stable defects implemented in popular processing and transport codes is facing an increasing number of problems. They can be attributed to discrepancies with measurements performed for the reactor irradiations [3–5], high energy ion irradiation [6], results of molecular dynamics (MD) simulations [7,8], and with results of new measurements [9–11]. It makes essential the calculation of displacement cross-sections using an advanced model, which predictions are in agreement with experimental data. The important feature of the model should be the ability to calculate the number of defects for a wide range of materials and kinetic energies of primary knock-on atoms (PKA), which is almost impossible today in MD simulations.

The athermal recombination-corrected dpa (arc-dpa) model [12,13] and the method of derivation of model parameters [14] meet all of the above criteria and make possible the use of results

of molecular dynamics simulations and available measured data for improved calculation of atomic displacement cross-sections for materials. The need for reliable radiation damage rate estimations gives particular importance to obtaining atomic displacement cross-sections using the model.

In the present work displacement cross-sections were calculated for materials from Be to Bi using the arc-dpa model [12–14], evaluated data files, nuclear models, and systematics. The cross-sections were obtained for primary neutron energy range from  $10^{-5}$  eV to 10 GeV covering the wide spectrum of possible applications. Without preference for any of evaluated data libraries, three sets of displacement cross-sections were obtained using JEFF-3.3 [15], ENDF/B-VIII [16], and JENDL [17] data at low energies. The TENDL files [18] and results of model calculations were applied for the extension of the data processed, as discussed below. The cross-sections obtained for aluminium, iron, copper, and tungsten supplement the corresponding data for proton induced reactions, recently evaluated for these materials [19].

Section 2 describes the method of calculation of displacement cross-sections and Section 3 discusses the evaluation procedure.

## 2. Method of calculation of displacement cross-sections

The displacement cross section is calculated using two independent types of models for calculating of recoil energy distributions and the number of stable displacements [20].

\* Corresponding author.

E-mail address: [alexander.konobeev@kit.edu](mailto:alexander.konobeev@kit.edu) (A.Yu. Konobeyev).

$$\sigma_d(E_n) = \sum_i \int_{E_d}^{T_i^{\max}} \frac{d\sigma(E_n, Z_T, A_T, Z_i, A_i, T_i)}{dT_i} N_d(Z_T, A_T, Z_i, A_i, T_i) dT_i \quad (1)$$

where  $E_n$  is the incident neutron energy;  $d\sigma/dT_i$  is the kinetic energy distribution of  $i$ -th PKA, where  $i$  refers to elastic scattering or nuclear reaction;  $Z$  and  $A$  are the atomic and the mass numbers, “ $T$ ” and “ $i$ ” relates to the target and the recoil atom, correspondingly;  $N_d$  is the number of stable defects produced;  $T_i^{\max}$  is the maximal kinetic energy of the  $i$ -th PKA; the summation is over all recoils produced by the irradiation.

Obtaining displacement cross sections, along with calculations, included a number of formal steps relating to the evaluation of cross-sections rather than to theoretical calculations: i) the processing of data from JEFF, ENDF/B, JENDL, and TENDL libraries; ii) the proper extension of obtained  $\sigma_d$  values up to 200 MeV, if necessary; iii) the correction of  $\sigma_d$  calculated using data libraries to avoid non-physical jumps and irregularities and ensuring a smooth data combination [21]; iv) the calculation of  $\sigma_d$  at neutron energies from several MeV to 10 GeV using nuclear models discussed below; v) the combination of data obtained in previous steps to get a global curve of  $\sigma_d$  from  $10^{-5}$  eV to 10 GeV in agreement with the applicability ranges of utilized nuclear models and evaluated data.

### 2.1. Recoil energy distributions

The NJOY code [22] was applied to calculate recoil spectra and displacement cross-sections using data from JEFF-3.3, ENDF/B-VIII, JENDL-4.0, and TENDL files.

The calculation of  $d\sigma/dT_i$  for nonelastic reactions of neutrons with nuclei at incident energies up to 10 GeV was performed using the CEM03.03 code [23].

Recoil energy distributions for neutron elastic scattering were calculated with the ECIS code [24] applying optical potentials from Refs. [25,26] and using the approximate approach from Ref. [27].

### 2.2. Number of stable displacements

According to the arc-dpa model the number of stable defects produced under irradiation is calculated as following [12,13].

$$N_d(T_{dam}) = \begin{cases} 0 & \text{when } T_{dam} < E_d \\ 1 & \text{when } E_d < T_{dam} < 2E_d/0.8 \\ \frac{0.8}{2E_d} \xi_{arc dpa}(T_{dam}) T_{dam} & \text{when } 2E_d/0.8 < T_{dam} \end{cases} \quad (2)$$

where  $T_{dam}$  is the energy available to produce atom displacement by elastic collision [1] calculated using the Robinson formula [2] (the “damage energy” [7]),  $E_d$  is the threshold displacement energy averaged over all lattice directions [4].

The defect generation efficiency  $\xi_{arc dpa}$  in Eq. (2) is approximated as follows [12,13].

$$\xi_{arc dpa}(T_{dam}) = \frac{1 - c_{arc dpa}}{(2E_d/0.8)^{b_{arc dpa}}} T_{dam}^{b_{arc dpa}} + c_{arc dpa} \quad (3)$$

where  $b_{arc dpa}$  and  $c_{arc dpa}$  are parameters.

The  $E_d$ ,  $b_{arc dpa}$ , and  $c_{arc dpa}$  values for materials from Be to Bi were taken from Refs. [12,14]. The preference was given to the Nordlund data [12], and if such data were missing for any element, the values obtained using systematics [14] were applied. In the latter case, the value of  $b_{arc dpa}$ , in contrast to Ref. [14], was taken equal to  $-0.82$  [21]. To obtain the  $\sigma_d$  values, consistent with displacement cross sections for proton irradiation for Al, Fe, Cu, and W [19], the calculations for these materials with arc-dpa model were corrected using the BCA model. Details are given in Ref. [19].

Eqs. (2) and (3) were directly implemented in NJOY [22] and CEM03 [23] codes.

Alternative calculations of  $\sigma_d$  values were performed using the NRT model [1,2] applying the same  $E_d$  values, as in the arc-dpa calculations.

## 3. Evaluation of displacement cross-sections

### 3.1. Use of evaluated data files at neutron energies up to 200 MeV

Data from JEFF-3.3 [15], ENDF/B-VIII [16], JENDL-4.0 [17], and TENDL files [18] were processed using the NJOY code applying the arc-dpa and NRT model to get displacement cross-sections.

As the first step to obtain displacement cross sections at all energies of interest, the data of the above libraries were extended up to the incident neutron energy 200 MeV using the TENDL data. A similar procedure was performed to get  $\sigma_d$  cross-sections included in DXS-2017 files [21,28]. For materials with atomic number above ten, the extension was performed using new TENDL-2017 files [18]. The  $\sigma_d$  values for light nuclei were enlarged using data prepared with earlier versions of TENDL [18], depending on the availability of evaluated data up to 200 MeV [29].

For most elements, the extension of  $\sigma_d$  was a “natural” continuation of the data and was not problematic. Fig. 1 shows typical examples.

### 3.2. Calculations at neutron energies up to 10 GeV

The contribution of neutron elastic scattering to displacement cross-section ( $\sigma_{d,el}$ ) was calculated using the ECIS code [24] and approximate formulas from Ref. [27].

The calculation with the ECIS code was performed using the Koning, Delaroche optical potential [25] at neutron energies from several MeV to 200 MeV and using the Madland potential [26] at

energies from 50 to 400 MeV according to the applicability range of potentials. The good agreement of results obtained with both potentials at neutron energies around 150–200 MeV to a certain extent simplified the estimation of  $\sigma_{d,el}$  cross sections at the energies from several MeV to 400 MeV (Fig. 2).

At higher energies the Sychev systematics [27] was used to calculate angular distributions for neutron elastic scattering and  $\sigma_{d,el}$  values. Similar approach is applied for the modelling with the MARS code [30].

When obtaining the full curve of elastic component of displacement cross-section, a preference at energies up to several

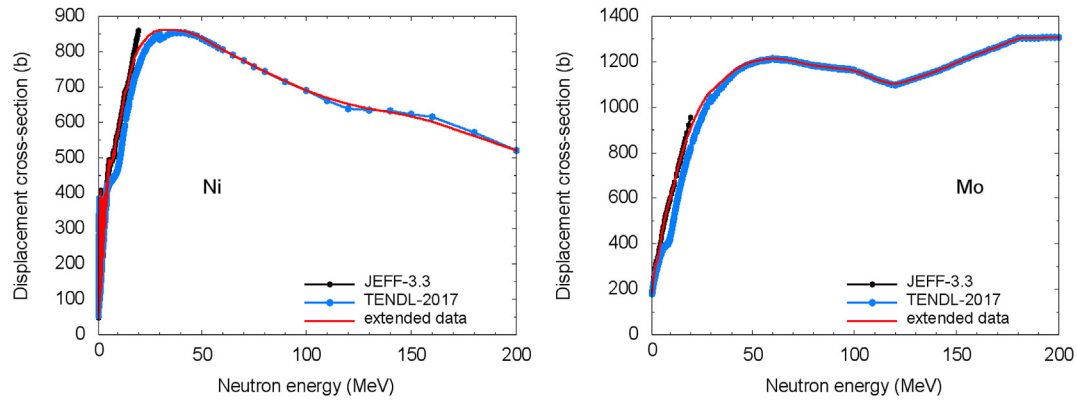


Fig. 1. Examples of the use of data prepared with TENDL-2017 for the extension of displacement cross-sections obtained using data from JEFF-3.3 up to 200 MeV.

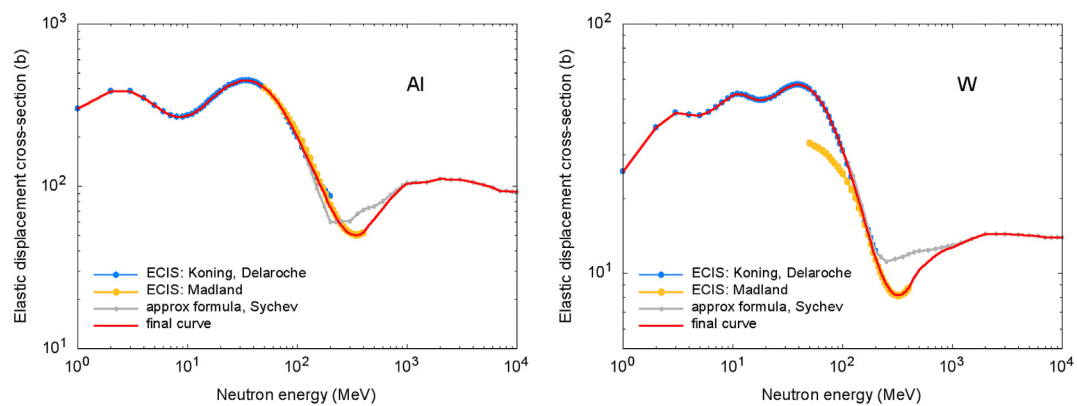


Fig. 2. Examples of displacement cross-sections for elastic scattering of neutrons calculated using the ECIS code with Koning, Delaroche [25] and Madland [26] optical potentials, displacement cross-sections estimated using approximate formulas [27], and the final evaluated curve.

hundred MeV was given to results of calculations with the optical model. Examples of the combination of  $\sigma_{d,el}$  cross sections calculated with ECIS and approximate formulas [27] are shown in Fig. 2. Apparently, the uncertainty of  $\sigma_{d,el}$  evaluation in the energy range of the “transition” from the optical model calculations to the systematics [27] (0.4–1 GeV, Fig. 2) does not have much influence on the total value of  $\sigma_d$  for most elements due to relatively small contribution of  $\sigma_{d,el}$  at these energies [31].

The contribution of neutron nonelastic interactions with nuclei to displacement cross-section was calculated using the CEM0.3 code [23] at incident neutron energies from several MeV to 10 GeV.

The code was adopted for calculations of displacement cross-sections and supplemented with corresponding routines and input variables.

Fig. 3 shows examples of calculated elastic and nonelastic components of displacement cross-sections for different materials.

### 3.3. Displacement cross-sections at energies from $10^{-5}$ eV to 10 GeV

Estimation of displacement cross sections in the entire energy range of interest was based on the proper combination of cross-sections obtained using evaluated data files ( $\sigma_{d1}$ ) (Sect. 3.1) and

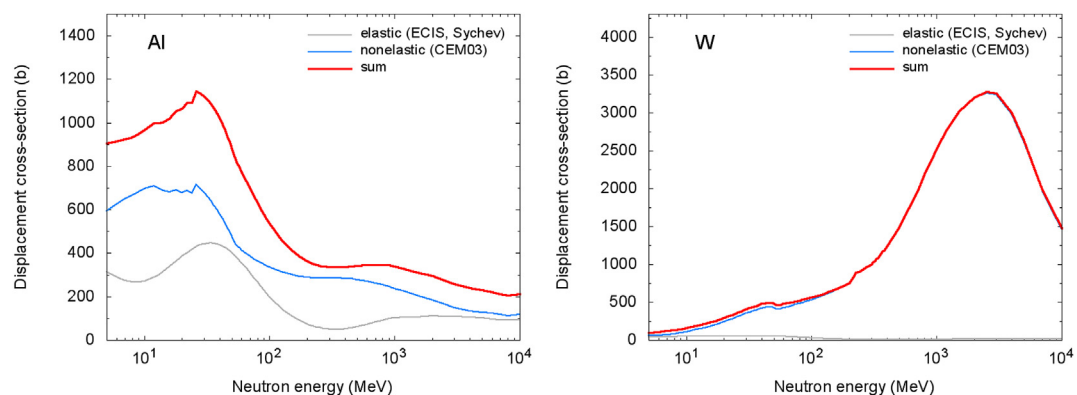


Fig. 3. Examples of calculated elastic and nonelastic components of displacement cross-sections.

the results of calculations with CEM03, ECIS, and systematics [27] ( $\sigma_{d2}$ ) (Sect. 3.2).

Evidently, at neutron incident energies below a few tens of MeV, the preference should be given to  $\sigma_{d1}$  cross-sections obtained from JEFF-3.3, ENDF/B-VIII, JENDL-4.0, and the TENDL data. As a rule, evaluated data, and in particular data from TENDL, were obtained using experimental data and results of calculations with advanced nuclear models, such as the pre-compound model [32], the Hauser-Feshbach model with the set of level density parameters obtained from the analysis of measured data [32]. With the growth of incident neutron energy, the uncertainty of predictions of such models increases, associated with both aspects of mathematical modelling of nuclear processes [32] and with applied systematics of pre-compound model parameters. At such energies, the advantages of the cascade-exciton model [33] implemented in CEM03, as well as Monte Carlo modelling, come to the fore [31].

The observed agreement between  $\sigma_{d1}$  and  $\sigma_{d2}$  at energies up to 50–150 MeV facilitates the combination of the data to get the displacement cross-section in the entire energy range from  $10^{-5}$  eV to 10 GeV (Fig. 4). Such combination was performed for displacement cross-sections calculated using both the arc-dpa and NRT model.

Displacement cross sections were obtained as discussed above for 79 materials from Be to Bi.

Fig. 5 shows the example of evaluated  $\sigma_d$  cross section for beryllium and iron. Values of  $\sigma_{d1}$  were calculated using data from JEFF-3.3.

Evaluated displacement cross sections were written in the ENDF-6 format and processed in the ACE format with the NJOY code. The data obtained can be downloaded on Ref. [34].

### 3.4. Estimation of uncertainty of displacement cross-sections

The estimation of the uncertainty of displacement cross sections including covariance information is a new challenging task and the part of the uncertainty assessment for radiation damage rate calculations for materials [35–38]. As a first step, in this paper data files containing covariance matrices for  $\sigma_d$  cross sections were prepared for a number of materials at neutron incident energies up to 200 MeV.

Analysis shows that the main source of uncertainty of  $\sigma_d$  cross sections is the spread of parameters of the arc-dpa model,  $E_d$ , and parameters of the NRT model [37,38]. The contribution of the uncertainty of reaction cross sections, resulted from the evaluation using experimental data and nuclear models, is relatively small [37]. As a preliminary estimate, the covariance matrices for reaction

cross-sections were taken from TENDL at energies up to 200 MeV.

The evaluation of covariance matrices for displacement cross-section was performed using the Monte Carlo (MC) method described in Ref. [39]. Some details can be found in Ref. [37]. Covariance matrices were obtained for displacement cross-sections calculated using both the arc-dpa model and NRT model. The procedure consisted in the MC sampling of total reaction cross-section, parameters of arc-dpa and NRT models, and subsequent calculation of displacement cross-sections [37].

In the calculations with the arc-dpa model, the sampling was performed for  $b_{arc-dpa}$  and  $c_{arc-dpa}$  parameters [37], and  $E_d$ , (Eq. (1),(2)). Other values, in particular, NRT “parameters” [38], were not changed. The calculation of displacement cross-sections using the NRT model was performed with the variation of  $E_d$  and parameters of the model discussed in Ref. [38]. The relative standard deviation value (RSD) for varied  $b_{arc-dpa}$ ,  $c_{arc-dpa}$ , and  $E_d$  was equal to 20% in all cases [37,38].

As an illustration, Fig. 6 shows calculated RSD values for displacement cross-sections for aluminium, titanium, and molybdenum.

Data obtained are written in the ENDF-6 format and can be downloaded on Ref. [40].

## 4. Conclusion

Displacement cross-sections were calculated for materials from Be to Bi using the arc-dpa model [12,13] and evaluated data from JEFF-3.3, ENDF/B-VIII, and JENDL-4.0. The  $\sigma_d$  cross-sections obtained were extended using the TENDL data up to incident neutron energy 200 MeV. In most cases, the extension was a “natural” continuation of the data, as discussed above.

The CEM03 code, the ECIS code and the systematics [27] were applied for calculations of displacement cross sections at energies from several MeV up to 10 GeV. The proper combination of cross-sections obtained using evaluated data files and calculations was performed taking into account the applicability of evaluation and calculation methods applied at different neutron incident energies. Three sets of  $\sigma_d$  cross-sections based on the use of low-energy data from JEFF-3.3, ENDF/B-VIII, and JENDL-4.0 were prepared.

The displacement cross-sections obtained at neutron energies from  $10^{-5}$  eV to 10 GeV can be downloaded on Ref. [34]. Files contain also  $\sigma_d$  cross-sections calculated using the NRT model.

Special efforts were made to estimate the uncertainty of evaluated displacement cross-sections. As the first step, the covariances matrices were obtained for a number of materials at neutron energies up to 200 MeV. Data are available in Ref. [40].

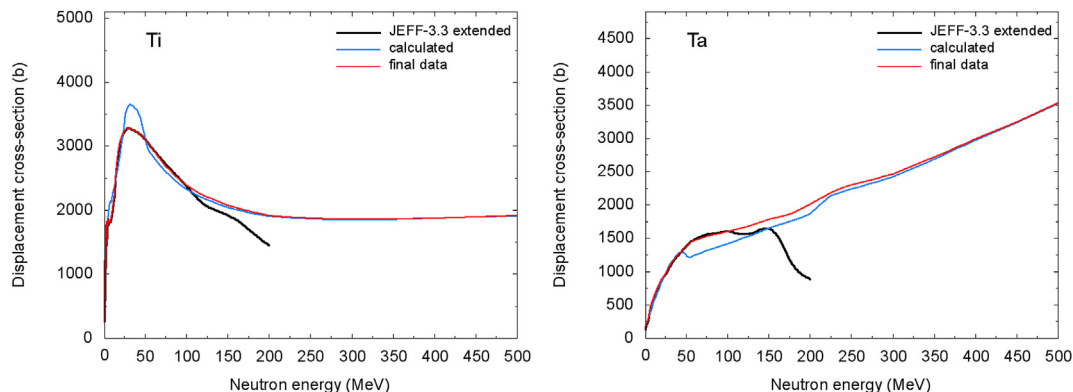


Fig. 4. Examples of displacement cross-sections obtained from the extension of JEFF-3.3 data, displacement cross-sections calculated using ECIS code, systematics [27], and CEM03 code (“calculated”) and evaluated cross-sections (“final data”).

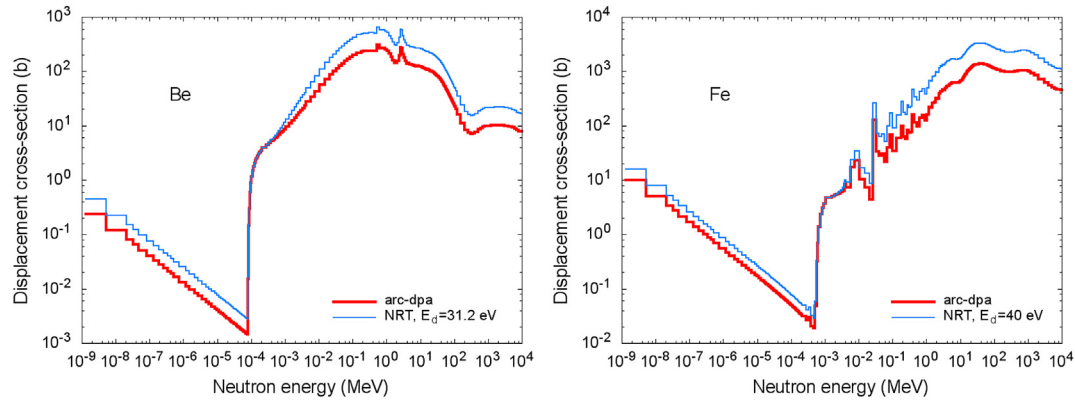


Fig. 5. Displacement cross-section for beryllium and iron obtained using the arc-dpa and NRT model. Values of  $\sigma_{d1}$  were calculated using data from JEFF-3.3 [15]. See explanations in the text.

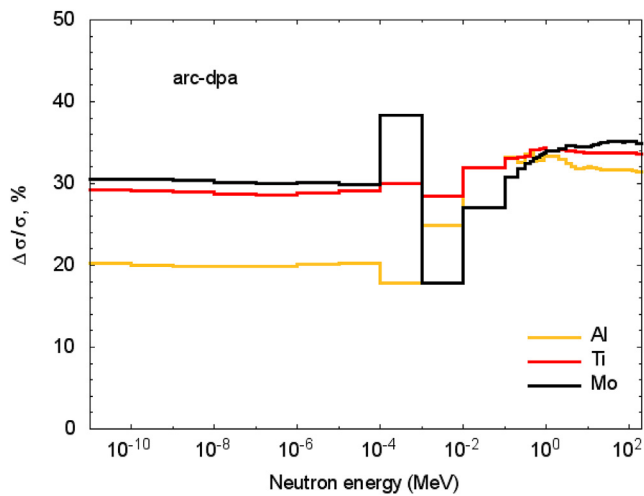


Fig. 6. Examples of estimated RSD values for displacement cross-sections. See explanations in the text.

Data obtained and displacement cross-sections calculated in Ref. [19] for proton induced reactions can be applied for improved evaluation of radiation damage rate in materials in a wide spectrum of nuclear facilities.

## Acknowledgment

This work has been partly funded from the EURATOM research and training programme 2014–2018 under grant agreement No 633053. The views and opinions expressed herein do not necessarily reflect those of the European Commission.

## References

- [1] M.J. Norgett, M.T. Robinson, I.M. Torrens, A proposed method of calculating displacement dose rates, *Nucl. Eng. Des.* 33 (1975) 50.
- [2] M.T. Robinson, Basic physics of radiation damage production, *J. Nucl. Mater.* 216 (1994) 1.
- [3] P. Jung, Atomic displacement functions of cubic metals, *J. Nucl. Mater.* 117 (1983) 70.
- [4] P. Jung, Production of atomic defects in metals, in: H. Ullmaier (Ed.), *Landolt-Börnstein, Group III: Crystal and Solid State Physics*, vol 25, Springer-Verlag, Berlin, 1991, p. 1.
- [5] C.H.M. Broeders, A.Yu Konobeyev, Defect production efficiency in metals under neutron irradiation, *J. Nucl. Mater.* 328 (2004) 197.
- [6] A. Dunlop, D. Lesueur, P. Legrand, H. Dammak, Effects induced by high electronic excitations in pure metals: a detailed study in iron, *Nucl. Instr. Meth. Phys. Res.* B90 (1994) 330.

- [7] K. Nordlund, A.E. Sand, F. Granberg, S.J. Zinkle, R. Stoller, R.S. Averback, T. Suzudo, L. Malerba, F. Banhart, W.J. Weber, F. Willaime, S. Dudarev, D. Simeone, *Primary Radiation Damage in Materials*, vol. 9, NEA/NSC/DOC, 2015. OECD (2015).
- [8] R.E. Stoller, L.R. Greenwood, S.P. Simakov (Eds.), *Primary Radiation Damage Cross Sections*, Summary Report of the Second Research Coordination Meeting, 29 June - 2 July 2015, IAEA, Vienna, December 2015, p. 19. INDC(NDS)-0691, <https://www-nds.iaea.org/publications/indc/indc-nds-0691.pdf>.
- [9] G.A. Greene, C.L. Snead Jr, C.C. Finckro, A.L. Hanson, M.R. James, W.F. Sommer, E.J. Pitcher, L.S. Waters, Direct measurements of displacement cross sections in copper and tungsten under irradiation by 1.10-GeV and 1.94-GeV protons at 4.7 K, Topical Meeting of the American Nuclear Society. Accelerator Applications in a Nuclear Renaissance (AccApp '03), 1-5 Jun 2003. San Diego.
- [10] Y. Iwamoto, T. Yoshiie, M. Yoshida, T. Nakamoto, M. Sakamoto, Y. Kuriyama, T. Uesugi, Y. Ishi, Q. Xu, H. Yashima, F. Takahashi, Y. Mori, T. Ogitsu, Measurement of the displacement cross-section of copper irradiated with 125 MeV protons at 12 K, *J. Nucl. Mater.* 458 (2015) 369.
- [11] Y. Iwamoto, M. Yoshida, T. Yoshiie, D. Satoh, H. Yashima, H. Matsuda, S.-i. Meigo, T. Shima, Measurement of displacement cross sections of aluminum and copper at 5K by using 200 MeV protons, *J. Nucl. Mater.* 508 (2018) 195, <https://doi.org/10.1016/j.jnucmat.2018.05.038>.
- [12] K. Nordlund, Summary of the 2nd RCM of CRP on primary radiation damage cross-section, in: Summary Report of the Second Research Coordination Meeting, 29 June - 2 July 2015, IAEA, Vienna, December 2015, p. 19. INDC(NDS)-0691, <https://www-nds.iaea.org/publications/indc/indc-nds-0691.pdf>.
- [13] K. Nordlund, S.J. Zinkle, A.E. Sand, F. Granberg, R.S. Averback, R. Stoller, T. Suzudo, L. Malerba, F. Banhart, W.J. Weber, F. Willaime, S.L. Dudarev, D. Simeone, Improving atomic displacement and replacement calculations with physically realistic damage models, *Nat. Commun.* 9 (2018) 1084, <https://doi.org/10.1038/s41467-018-03415-5>.
- [14] A.Yu Konobeyev, U. Fischer, YuA. Korovin, S.P. Simakov, Evaluation of effective threshold displacement energies and other data required for the calculation of advanced atomic displacement cross-sections, *Nucl. Energy Technol.* 3 (2017) 169.
- [15] The Joint Evaluated Fission and Fusion File. JEFF-3.3, 2018. <http://www.oecd-nea.org/dbdata/jeff/jeff33/index.html>.
- [16] D.A. Brown, M.B. Chadwick, R. Capote, A.C. Kahler, A. Trkov, M.W. Herman, A.A. Sonzogni, Y. Danon, A.D. Carlson, M. Dunn, D.L. Smith, G.M. Hale, G. Arbanas, R. Arcilla, C.R. Bates, B. Beck, B. Becker, F. Brown, R.J. Casperson, J. Conlin, D.E. Cullen, M.-A. Descalle, R. Firestone, T. Gaines, K.H. Guber, A.I. Hawari, J. Holmes, T.D. Johnson, T. Kawano, B.C. Kiedrowski, A.J. Koning, S. Kopecky, L. Leal, J.P. Lestone, C. Lubitz, J.I. Márquez Damián, C.M. Mattoon, E.A. McCutchan, S. Mughabghab, P. Navratil, D. Neudecker, G.P.A. Nobre, G. Noguere, M. Paris, M.T. Pigni, A.J. Plompen, B. Pritychenko, V.G. Pronyaev, D. Roubtsov, D. Rochman, P. Romano, P. Schillebeeckx, S. Simakov, M. Sin, I. Sirakov, B. Sleaford, V. Sobes, E.S. Soukhovitskii, I. Stetcu, P. Talou, I. Thompson, S. van der Marck, L. Welser-Sherill, D. Wiarda, M. White, J.L. Wormald, R.Q. Wright, M. Zerckle, G. Žerovnik, Y. Zhu, ENDF/B-VIII.0: the 8<sup>th</sup> major release of the nuclear reaction data library with CIELO-project cross sections, new standards and thermal scattering data, *Nucl. Data Sheets* 148 (2018) 1. ENDF/B-VIII.0 (2018), <http://www.nndc.bnl.gov/ndf/b8.0/>.
- [17] Japanese Evaluated Nuclear Data Library. JENDL, 2018. <https://www.ndc.jaea.go.jp/jendl/jendl.html>.
- [18] D. Rochman, A.J. Koning, J.Ch Sublet, M. Fleming, E. Bauge, S. Hilaire, P. Romain, B. Morillon, H. Duarte, S. Goriely, S.C. van der Marck, H. Sjöstrand, S. Pomp, N. Dzysiuk, O. Cabellos, H. Ferroukhi, A. Vasiliev, The TENDL Library: hope, reality and future, in: EPJ Web of Conferences, vol 146, 2017, <https://doi.org/10.1051/epjconf/201714602006>, 02006.

- [19] A.Yu Konobeyev, U. Fischer, S.P. Simakov, Improved atomic displacement cross-sections for proton irradiation of aluminium, iron, copper, and tungsten at energies up to 10 GeV, *Nucl. Instrum. Meth. Phys. Res. B* 431 (2018) 55. Numerical data are available: <https://www.inr.kit.edu/english/779.php>.
- [20] A.Yu Konobeyev, U. Fischer, P.E. Pereslavl'tsev, S.P. Simakov, S. Akca, Evaluated displacement and gas production cross-sections for materials irradiated with intermediate energy nucleons, *EPJ Web Conf.* 146 (2017), 02018, <https://doi.org/10.1051/epjconf/201714602018>.
- [21] A.Yu Konobeyev, U. Fischer, S.P. Simakov, Neutron displacement cross-sections for materials from Be to U calculated using the arc-dpa concept, *Proc. 13th International Topical Meeting on the Applications of Accelerators (AccApp'17)*, July 31-August 4, 2017, Quebec, <http://accapp17.org/wp-content/2017/data/pdfs/110-22892.pdf>; <https://goo.gl/3swcvs>.
- [22] D.W. Muir, R.M. Boicourt, A.C. Kahler, *The NJOY Nuclear Data Processing System, Version 2012*, LA-UR-12-27079 Rev, February 2015.
- [23] S.G. Mashnik, A.J. Sierk, CEM03.03 User Manual, Report LA-UR-12-01364, 2012.
- [24] J. Raynal, in: "ECIS96," *Proc. Specialists' Meeting on the Nucleon Nucleus Optical Model up to 200 MeV*, Bruyères-le-Chatel, France, Nov. 13-15, 1996. <http://www.nea.fr/html/science/om200/raynal.pdf>.
- [25] A.J. Koning, J.P. Delaroche, Local and global nucleon optical models from 1 keV to 200 MeV, *Nucl. Phys. A* 713 (2003) 231.
- [26] D.G. Madland, Progress in the development of global medium-energy nucleon-nucleus optical model potentials, in: *Proc. Spec. Meeting on the Nucleon Nucleus Optical Model up to 200 MeV*, Bruyères-le-Chatel, November 13-15, 1996, p. 129.
- [27] B.S. Sychev, *Cross Sections of High Energy Hadron Interactions on Nuclei*, Russian Academy of Sciences, Moscow Radiotechnical Institute, Moscow, 1999.
- [28] DXS-2017 (2017), <https://www-nds.iaea.org/JEFF-3.3dpa> sublibrary (2017), <http://www.oecd-nea.org/dbdata/jeff/jeff33/#dpa>.
- [29] A.Yu Konobeyev, U. Fischer, P.E. Pereslavl'tsev, S.P. Simakov, in: *Arc-dpa Cross-sections for High Priority Elements*, JEFF Meeting, 20 – 24, November 2017, <https://doi.org/10.13140/RG.2.2.32203.0848>. EFFDOC-1338, <https://goo.gl/xMbEVn>, [http://www.oecd-nea.org/dbdata/nds\\_effdoc/effdoc-1338.pdf](http://www.oecd-nea.org/dbdata/nds_effdoc/effdoc-1338.pdf).
- [30] I. Rakhno, N. Mokhov, E. Sukhovitski, S. Chiba, Simulation of Nucleon Elastic Scattering in the MARS14 Code System, November 2001. FERMILAB-Conf-01/343-T.
- [31] A.Yu Konobeyev, U. Fischer, S.P. Simakov, in: *Improved Displacement Cross-sections for Neutron Irradiation of Materials from Be to U*, JEFF Meeting, 18 – 20 April, 2018, <https://doi.org/10.13140/RG.2.2.25085.87524>. EFFDOC-1350, <https://goo.gl/4Lb3e6>.
- [32] A. Koning, S. Hilaire, S. Goriely, TALYS-1.9. A Nuclear Reaction Program. User Manual, 2017. <http://www.talys.eu/download-talys/>.
- [33] S.G. Mashnik, A.J. Sierk, Recent developments of the cascade-exciton model of nuclear reactions, *J. Nucl. Sci. Technol.* 2 (2002) 720.
- [34] Evaluated Displacement Cross-sections for Neutron Induced Reactions, 2018. <https://www.inr.kit.edu/english/779.php>. <https://goo.gl/yad96Z>.
- [35] S.P. Simakov, A. Koning, A.Yu Konobeyev, Covariances for the  $^{56}\text{Fe}$  radiation damage cross sections, in: *EPJ Web of Conferences*, vol 146, 2017, 02012, <https://doi.org/10.1051/epjconf/201714602012>.
- [36] S.P. Simakov, U. Fischer, A.J. Koning, A.Yu Konobeyev, D.A. Rochman, Iron NRT- and arc-displacement cross sections and their covariances, *Nucl. Mater. Energy* 15 (2018) 244.
- [37] A.Yu Konobeyev, U. Fischer, S.P. Simakov, Uncertainties of displacement cross-sections for iron and tungsten at neutron irradiation energies above 0.1 MeV, *KIT SWP* 49, <http://digbib.ubka.uni-karlsruhe.de/volltexte/1000057548>, 2016.
- [38] A.Yu Konobeyev, U. Fischer, S.P. Simakov, Uncertainty assessment for the number of defects calculated using the NRT damage model, *KIT SWP* 70, <https://publikationen.bibliothek.kit.edu/1000074095>, 2017.
- [39] D.L. Smith, Covariance Matrices for Nuclear Cross Sections Derived from Nuclear Model Calculations, Argonne National Laboratory, 2004. ANL/NDM-159.
- [40] Evaluated Displacement Cross-sections for Neutron Induced Reactions with Covariances, 2018. <https://www.inr.kit.edu/english/779.php>. <https://goo.gl/u4ph5u>.